

Proposal to the INTC Committee

Study of the onset of deformation and shape coexistence in ^{46}Ar via the inverse kinematics (t,p) reaction

K. Wimmer¹, R. Krücken¹, V. Bildstein¹, T. Faestermann¹, R. Gernhäuser¹, D. Habs², P. Thirof², R. Lutter², L. Csige², P. Van Duppen³, R. Raabe¹⁹, N. Patronis¹⁸, N. Bree³, M. Huyse³, J. Elseviers³, J. Diriken³, J. Van de Walle⁴, J. Pakarinen⁴, E. Clement¹⁹, J. Cederkäll⁴, D. Voulot⁴, T. Stora⁴, F. Wenander⁴, L. M. Fraile⁵, T. Davinson⁶, P. J. Woods⁶, T. Nilsson⁷, E. Tengborn⁷, R. Chapman⁸, J. F. Smith⁸, L. Angus⁸, M. Labiche¹⁷, P. Wady⁸, D. Jenkins⁹, J. Butterworth⁹, B. S. Nara Singh⁹, S. Freeman¹⁰, C. Fitzpatrick¹⁰, A. Deacon¹⁰, P. Butler¹¹, M. Scheck¹¹, A. Blazhev¹², N. Warr¹², P. Reiter¹², M. Seidlitz¹², G. Georgiev¹³, E. Fiori¹³, R. Lozeva¹³, Th. Kröll¹⁴, N. Pietralla¹⁴, G. Schrieder¹⁴, D. Balabanski¹⁵, G. Lo Bianco¹⁶, S. Das Gupta¹⁶, S. Nardelli¹⁶, A. Görge²⁰, W. Korten²⁰, A. Obertelli²⁰, K. Hadynska-Klek²¹, J. Iwanicki²¹, P. J. Napiorkowski²¹, J. Srebrny²¹, K. Wrzosek-Lipska²¹, M. Zielińska²¹ and the REX-ISOLDE and MINIBALL collaborations

¹Physik-Department E12, Technische Universität München, Garching, Germany, ²Fakultät für Physik, Ludwig-Maximilians-Universität München, Garching, Germany, ³Instituut voor Kern- en Stralingsfysica, Katholieke Universiteit Leuven, Belgium, ⁴CERN, Genève, Switzerland, ⁵Dpto. de Física Atómica, Molecular y Nuclear, Universidad Complutense, Madrid, Spain, ⁶Department of Physics and Astronomy, University of Edinburgh, Scotland, UK, ⁷Fundamental Fysik, Chalmers Tekniska Högskola, Göteborg, Sweden, ⁸School of Engineering and Science, Univ. of the West of Scotland, Paisley, Scotland, UK, ⁹Nuclear Physics Group, Department of Physics, University of York, UK, ¹⁰Nuclear Physics Group, Schuster Laboratory, University of Manchester, UK, ¹¹Oliver Lodge Laboratory, University of Liverpool, UK, ¹²Institut für Kernphysik, Universität zu Köln, Germany, ¹³Centre de Spectrométrie Nucléaire et de Spectrométrie de Masse, Orsay, France, ¹⁴Institut für Kernphysik, Technische Universität Darmstadt, Germany, ¹⁵INRNE, Bulgarian Academy of Sciences, Sofia, Bulgaria, ¹⁶Dipartimento di Fisica, Università di Camerino, Italy, ¹⁷Daresbury Laboratory, Warrington, UK, ¹⁸Department of Physics, The University of Ioannina, Greece, ¹⁹GANIL, Caen, France, ²⁰CEA/Saclay, Irfu/SPhN, Gif-sur-Yvette, France, ²¹Heavy Ion Laboratory, University of Warsaw, Poland

Abstract: We plan to study states in ^{46}Ar via the (t,p) two-neutron transfer reaction in inverse kinematics in order to identify and characterize excited states and to gain insights into the onset of deformation and the possible occurrence of shape-coexistence in this region where the $N = 28$ shell closure may be weakening. The experiment will be performed using accelerated beams from REX-ISOLDE and the T-REX particle detector set-up inside MINIBALL. We request a total of 30 shifts + 3 shifts for beam commissioning.

Spokesperson: K. Wimmer

Contact person: J. Pakarinen



1 Physics case

The evolution of the $N = 28$ shell gap below ^{48}Ca has been the subject of a large number of theoretical and experimental studies (see Ref. [1] for a recent review). Only four protons below $^{48}_{20}\text{Ca}$ the $N = 28$ nucleus $^{44}_{16}\text{S}$ exhibits a 2^+ energy and $B(E2)$ value consistent with a configuration intermediate between spherical and deformed. This has been interpreted as a possible sign for the mixing of spherical and deformed shapes in $^{44}_{16}\text{S}$ and preliminary evidence has been reported for a long lived 0^+ state in Ref. [2]. For ^{42}Si some available experimental information indicates that this nucleus is well deformed. However, there is conflicting experimental evidence and more information certainly is needed.

The development of deformation in the $N = 28$ isotones has been attributed mostly to the disappearance of the spacing of the proton $d_{3/2}$ and $s_{1/2}$ single-particle levels as the neutron $f_{7/2}$ level is filled. Collectivity can easily arise from the long range quadrupole interaction between these orbitals. At the same time there are indications of a slight reduction of the $N = 28$ shell gap which would provide additional incentives for deformation.

In the neutron-rich Ar isotopes the single-particle structure of ^{45}Ar was investigated at GANIL using the $^{44}\text{Ar}(d, p)$ reaction [3]. A significant fragmentation of spectroscopic strength was observed for the low-lying states which are attributed to core excitations of $1p - 2h$ nature, as compared to the $0p - 1h$ structure of the closed shell configuration. Excited states in ^{46}Ar were observed in intermediate energy Coulomb excitation [4], secondary fragmentation [5], and inelastic proton scattering [6] but only the first excited 2^+ state has been firmly established. The most neutron-rich Ar isotopes for which excited states have been observed are ^{47}Ar and ^{48}Ar , which were populated in deep inelastic collisions [7]. While all spin assignments in $^{47,48}\text{Ar}$ are tentative, the comparison to shell model calculations suggests that particle-hole excitations across the $N = 28$ shell gap play a significant role for the excited states in all Ar isotopes near $N = 28$.

A recent lifetime measurement in $^{44,46}\text{Ar}$ using the RDDS plunger method [8] came to the conclusion that there are indications of a $N = 28$ weakening. In addition a most recent study of excited states in ^{44}Ar via low-energy Coulomb excitation at SPIRAL (GANIL) [9] found a negative value for the quadrupole moment of the first excited 2^+ state in this nucleus, thus suggesting a prolate deformation. The results were compared to shell-model and relativistic mean-field calculations and to both axial and triaxial configuration mixing calculations using the generator coordinate method with the Gogny D1S interaction. None of the models is able to fully reproduce energies as well as $B(E2)$ values. More experimental information is clearly needed to understand the onset of deformation and the possible occurrence of shape coexistence in this region.

According to shell model calculations the low-lying states in ^{46}Ar exhibit significant $2p - 2h$ character. However, only the ground state and the first excited 2^+ state have firm spin assignments. A state observed at 2710 keV, which decays only to the first excited 2^+ state, has been suggested to be a candidate for the predicted $2p - 2h$ shape coexisting 0^+ state [5]. Only a few other states have been observed between 2.7 MeV and 5 MeV [5, 6]. **Motivated by these considerations we propose to study excited states in ^{46}Ar at REX-ISOLDE using the two-neutron transfer (t, p) reaction. We hope to establish new excited states and get firm spin assignments of both known and new states in ^{46}Ar . In addition we will use the relative population of levels**

to obtain information on configuration mixing by comparison to theoretical calculations. In particular, the $2p - 2h$ 0^+ state in ^{46}Ar is expected to be populated strongly, enabling its identification.

2 Experimental method

We propose to utilize the $t(^{44}\text{Ar}, p)$ two-neutron transfer reactions in inverse kinematics to populate states in ^{46}Ar . We will detect emitted protons in our new charged particle array T-REX [10], which was successfully used in our previous $t(^{30}\text{Mg}, p)^{32}\text{Mg}$ experiment IS470.

The energies and angular distributions of the emitted protons will be used to identify the transferred angular momentum and thus the spins of the final states. Since the energy separation of the known states in ^{46}Ar is quite large, the energy levels can be separated by the proton energies alone. In addition the observation of decay γ rays with MINIBALL from the excited states may yield additional important information.

The measured cross sections and angular distributions will be analyzed in the framework of the DWBA by applying the code FRESKO [11]. The optical potentials needed for this analysis can be obtained by scaling the values obtained in stable-beam scattering experiments to the mass of the projectile and the beam energy [12]. The optical model parameters can be pinned down also from the analysis of the (t, d) reaction and the elastically scattered tritons.

The results of such an analysis are the excitation energy, the transferred orbital momentum and the relative strength with which the states are populated.

2.1 Previous (t, p) experiments

Due to the experience we have gained from our successful study of the $t(^{30}\text{Mg}, p)^{32}\text{Mg}$ reaction at REX-ISOLDE (IS470) we are confident about the successful outcome of the proposed experiment. In this study two states in ^{32}Mg were populated, the ground state and a new excited state at around 1.1 MeV, which shows the characteristic angular distribution of a 0^+ state (see Fig. 1). This new 0^+ state can be identified as the predicted coexisting spherical $0p-0h$ state in ^{32}Mg which is deformed in its ground state.

In addition we have performed a stable beam (t, p) test experiment using ^{40}Ar beam at 2.25 MeV/u and $6 \cdot 10^8$ part/s at the HMI (Berlin). This reaction was studied previously in forward kinematics by Flynn et al. [14]. Fig. 2 shows an energy spectrum of one detector ring from our inverse kinematics-experiment. In this reaction with a Q-value of 7.04 MeV states from the ground state up to 6.5 MeV were populated and observed. At high energies however the states could not be resolved solely from the particle energies, and gamma ray detection would have proven very beneficial. Figure 3 shows the angular distributions from transfer to several states in ^{42}Ar . Even with the limited angular coverage of the set-up used in the test experiment the characteristic $\Delta L = 0$ angular distribution for the ground state could be clearly distinguished. For larger angular momentum transfer the distributions are rather flat and a larger angular coverage is essential to identify the transferred angular momentum.

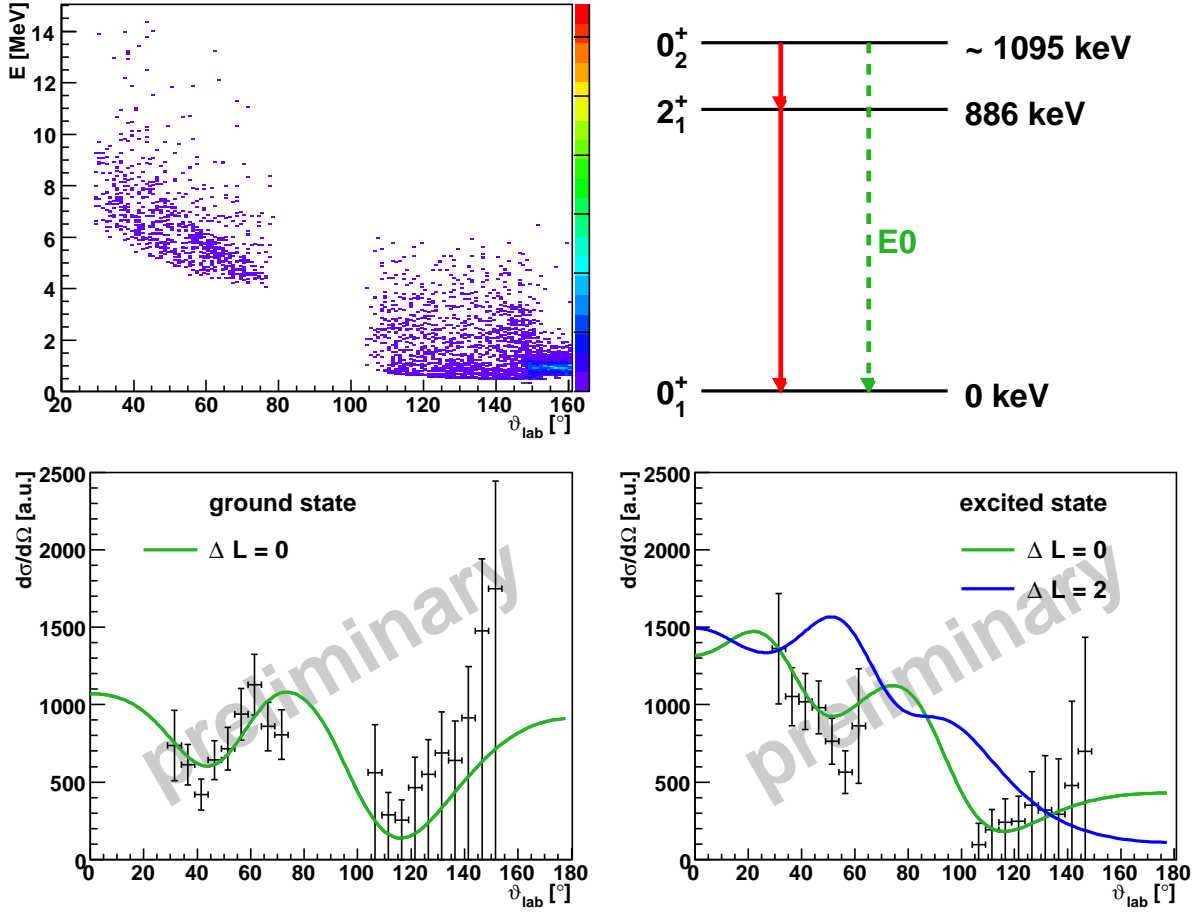


Figure 1: a) $E - \vartheta_{\text{lab}}$ spectrum. The two states can be separated in forward direction. b) proposed level scheme of ^{32}Mg with the new state around 1.1 MeV. c) and d) angular distribution in the laboratory system for the two states compared with DWBA calculations.

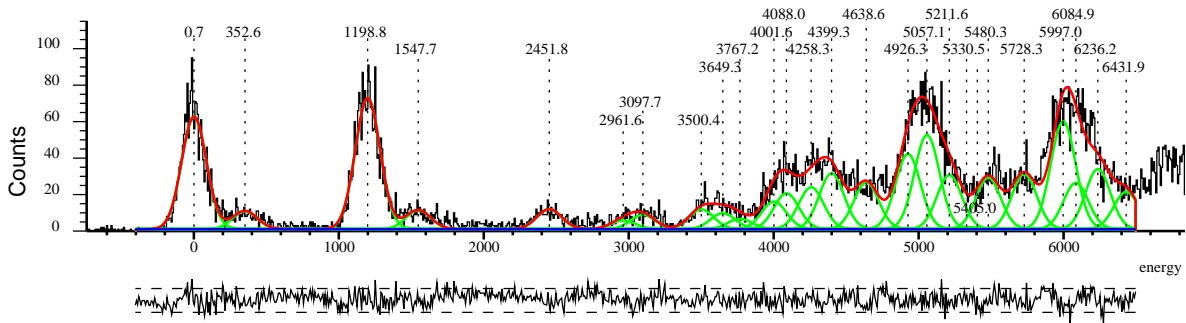


Figure 2: Spectrum of a single ring of the DSSSD, ring 10, from the reaction $t(^{40}\text{Ar}, p)^{42}\text{Ar}$ at $E_{^{40}\text{Ar}}^{\text{lab}} = 2.16$ MeV/u. The lower part of the figure shows the difference between the fit and the data, normalized with the error of the data. (taken from Ref. [13])

This stable beam experiment was also important for the monitoring of the stability of the

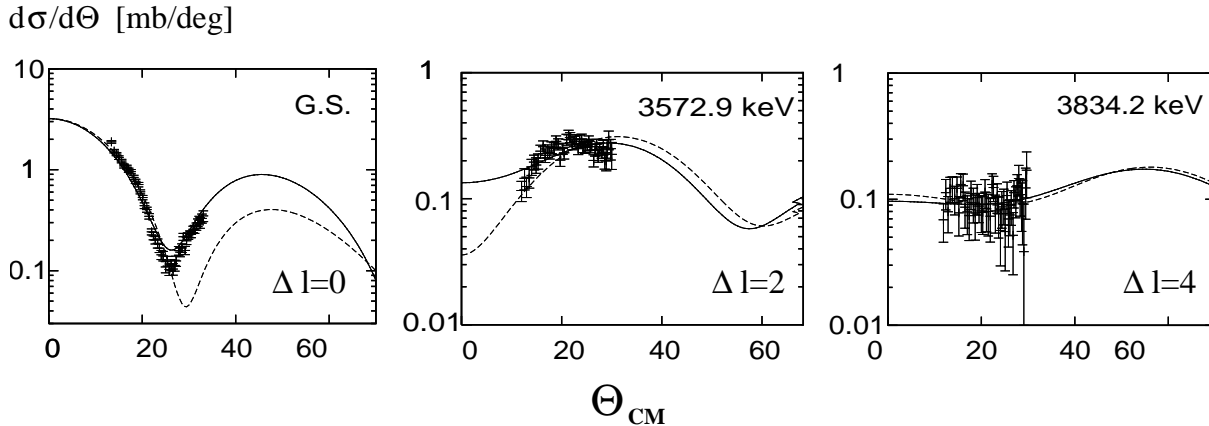


Figure 3: Examples for experimental and calculated cross sections for the protons emitted from the reaction ${}^3\text{H}({}^{40}\text{Ar}, {}^{42}\text{Ar}){}^1\text{H}$ at 2.25 MeV/u [13].

tritium target. The rate of scattered tritium nuclei was monitored during the whole run. No reduction indicating a loss of material in the target has been observed. Additionally, after the experiment the filter in front of the vacuum pumps exhibited no radioactivity. Also in the $t({}^{30}\text{Mg}, p){}^{32}\text{Mg}$ experiment no problems were encountered with the tritium target.

2.2 Experimental set-up

The set-up consists of our T-REX (see Fig. 4) charged particle array of segmented Si detectors [10] with about 60% solid angle coverage surrounded by the MINIBALL array to detect γ rays in coincidence with particles. The T-REX set-up was successfully used in the $d({}^{30}\text{Mg}, p)$ and $t({}^{30}\text{Mg}, p)$ transfer experiments (IS454, IS470).

The T-REX array comprises two double-sided segmented Si detectors (DSSSD), so-called CD detectors, in forward and backward direction and a barrel of eight planar detectors around 90° . The forward CD detector consists of two layers providing a $\Delta E - E$ -telescope. The ΔE -detector (thickness $300 \mu\text{m}$) has four quadrants, each of them is segmented in 16 annular stripes (ϑ -coordinate) on the front and in 24 radial segments (ϕ -coordinate) on the back. The E -detector (thickness $1500 \mu\text{m}$) is segmented only in 4 quadrants. The backward CD detector has the same segmentation as the forward ΔE -detector, but a thickness of $500 \mu\text{m}$. The eight detectors of the barrel are also $\Delta E - E$ -telescopes. The ΔE -detector (thickness $140 \mu\text{m}$) is segmented in 16 stripes perpendicular to the beam axis. Positional information along the stripes can be obtained from the charge division on a resistive layer. The E -detector is not segmented and has a thickness of $1000 \mu\text{m}$.

The use of $\Delta E - E$ -telescopes in forward direction enables the identification of light particles (p,d,t, α). The energy resolution for excitation energies ranges from 250 keV to 2 MeV depending on angle and energy. The angular resolution is typically below 5° .

In order to reduce the high count rate from elastic scattering of both Ar beam and target nuclei, i.e. tritons and Ti, Mylar foils are mounted in front of the forward detectors. These foils stop all heavy ions, but the tritons only around 90° . Since the beam particles are

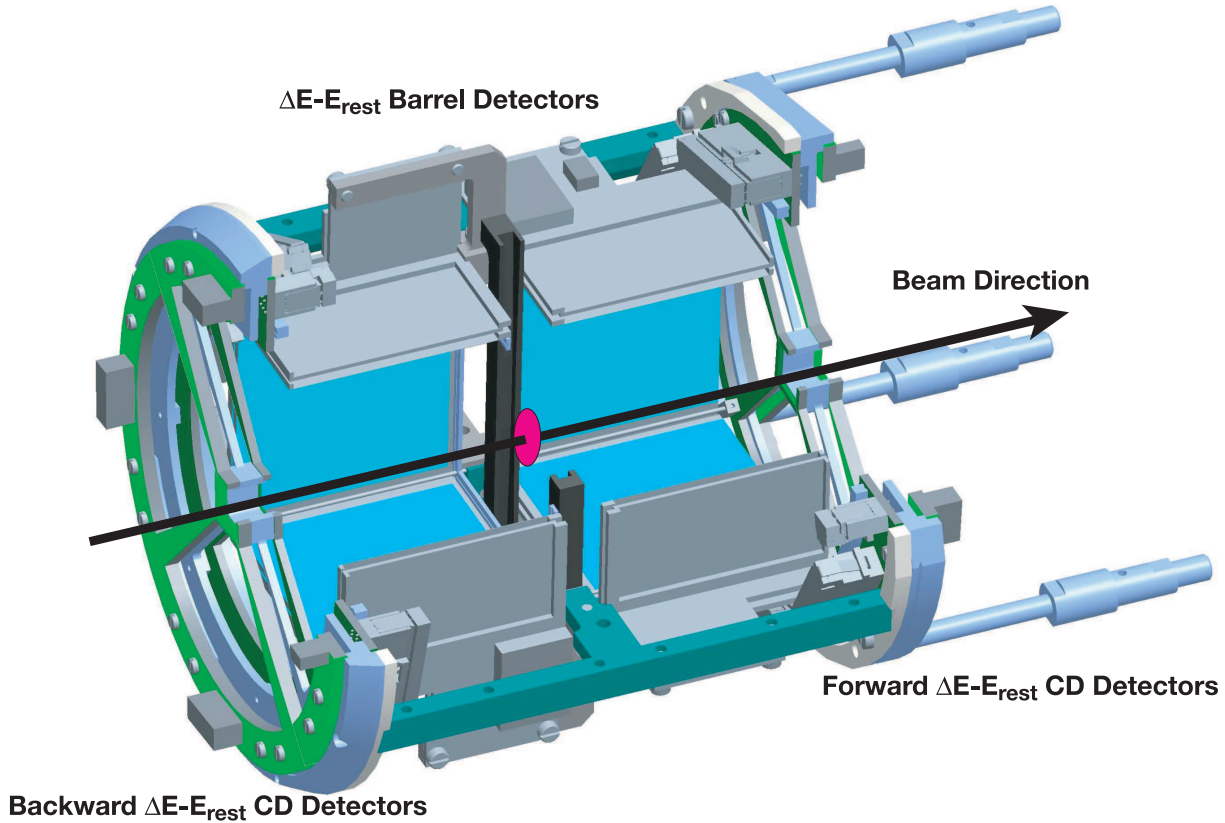


Figure 4: T-REX Si detector with eight barrel detectors and 2 CDs.

lighter than the target carrier material Titanium, Ar can also be scattered in backward directions. Since in backward direction particle identification is not possible, these beam particles have to be stopped in an additional Mylar foil in the backward direction.

2.3 Beam production and composition

The highest production yields for ^{44}Ar are reported for a UC_x /graphite target coupled via a cold transfer line to a MK7 hot plasma ion source, with production yields of $\approx 3 \cdot 10^6$ atoms/ μC . However, with the new VADIS ion source [15] the yields for noble gases are by a factor of 3 higher. Due to the cooled transfer line the only atomic contaminations are higher charged nobles gases, $^{86}\text{Kr}^{++}$ and $^{132}\text{Xe}^{+++}$ which will be cleaned up in the REX-TRAP. There will however be a considerable amount of CO_2 from the ion source in the beam, which can overload the REX-TRAP. Depending on the actual yields for ^{44}Ar the beam could be continuously injected to the EBIS without cooling in the REX-TRAP. This would lower the total transmission efficiency to $\approx 2 - 3\%$ compared to the normal configuration with $\approx 5\%$ total efficiency. Alternatively the VADIS ion source could be operated at a lower temperature which significantly reduces the CO_2 content of the beam. The CO_2 molecule will be broken in the EBIS and does not contaminate the beam at MINIBALL. ^{22}Ne with the same A/q from the buffer gas can be avoided by using isotopically enriched ^{20}Ne as it was used for the ^{11}Be beam in IS430. Despite

these disadvantages, a minimum beam intensity of 10^5 part/s at the T-REX setup can be expected.

For beam focusing a segmented diamond detector on the target ladder which can be moved to the target position and an active collimator with four PIN diodes in front of the chamber have been included.

2.4 Radioactive ^3H target

The proposed experiment is only possible with the unique combination of a radioactive beam with a radioactive target, in our case a tritium-loaded Ti foil.

We have safely and successfully used a tritium-loaded Ti foil in the REX-ISOLDE experiment IS470 for the study of the reaction $t(^{30}\text{Mg}, p)^{32}\text{Mg}$. The target is based on a thin strip of $500 \mu\text{g}/\text{cm}^2$ thick metallic Ti foil loaded with a atomic ratio $^3\text{H}/\text{Ti}$ of 1.5 corresponding to a target thickness of $40 \mu\text{g}/\text{cm}^2$ ^3H . With an activity of less than 10 GBq the target handling at ISOLDE was permitted following CERN Specification N° 4229RP20070405-GD-001 [16]. In the proposed experiment we will either use the same target or purchase a new one of identical make.

3 DWBA calculations and simulations

In order to avoid fusion with the target carrier material Ti the beam energy has to be lowered to 2.16 MeV/u from the maximum REX beam energy of 2.85 MeV/u.

We have performed DWBA calculations using the code FRESKO [11] using global optical model parameters extrapolated from stable nuclei [17], scaled to the lower beam energy. Due to the large positive Q-value for the (t, p) reaction to the ground state of ^{46}Ar of 4.7 MeV [18], states at higher excitation energy are somewhat favored in the reaction and our experience from the $t(^{40}\text{Ar}, p)^{42}\text{Ar}$ reaction shows that many states can be populated. For ^{46}Ar we have used the energies of the known levels and the suggested spin assignments (the level scheme is shown in Fig. 5 of Reference [5]) to calculate the angular distributions of the emitted protons shown in Fig 5 a). We have assumed spectroscopic factors of one for all transitions. This is a reasonable assumption (at least for the 0^+ states) from the experimental results of the $t(^{30}\text{Mg}, p)$ and $t(^{40}\text{Ar}, p)$ reactions. These distributions were used as input for GEANT4 [19] simulations of the expected light charged particle emissions and the expected detector response of the T-REX set-up. Figure 5 b) shows the proton energies as a function of laboratory angle for the $t(^{44}\text{Ar}, p)^{46}\text{Ar}$ reaction indicating that a clear separation of the known states is possible on the basis of the proton energies alone.

Protons from this reaction can be easily detected due to their high energy, which also enables their identification by $\Delta E - E$ separation in the Si-Telescopes of the T-REX set-up. The competing (t, d) reaction channel has a Q-value of -1.1 MeV and because of the negative Q-value and mass transfer from the target nuclei the deuterons will only be observed in forward direction in the laboratory system. They can be distinguished from the protons by using the $\Delta E - E$ separation.

With the high Q-value of 4.7 MeV for the (t, p) reaction, the proton energy in backward

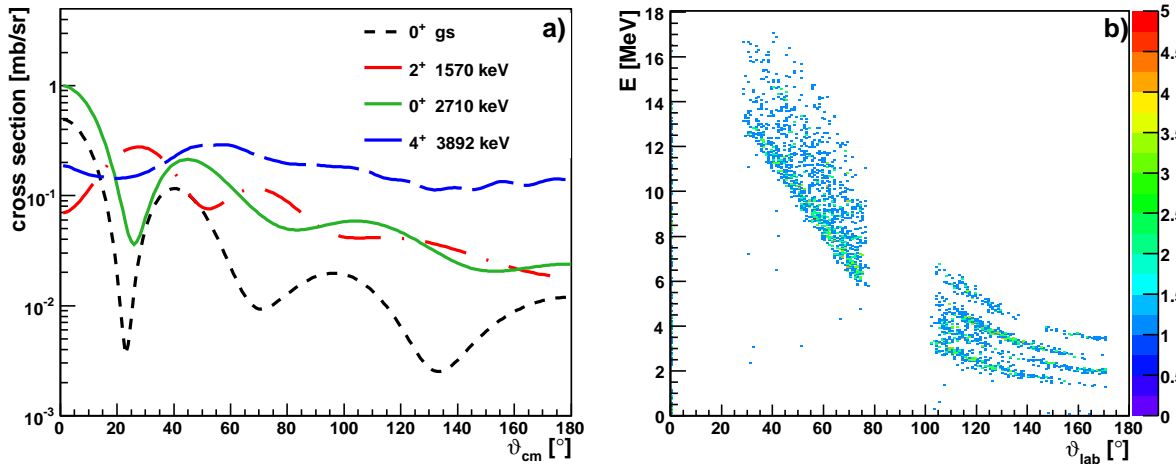


Figure 5: a) Angular distributions of protons emitted in the $t(^{44}\text{Ar}, p)^{46}\text{Ar}$ reaction. b) Proton energy as a function of laboratory angle. The number of simulated events corresponds to the expected number of counts.

direction is sufficient to punch through the ΔE -detector up to $\approx 130^\circ$ for low lying states. This allows for an additional suppression of the β electrons. Because of their high energy the protons in backward direction can be easily detected as compared to the IS470 experiment where part of the protons are below the detection threshold.

With the anticipated yields for the experiment (see below) we should be able to uniquely identify the spins of the different states from their angular distributions.

4 Rate estimate and beam time request

The DWBA calculations for the $t(^{44}\text{Ar}, p)^{46}\text{Ar}$ indicate comparable cross sections to the ones predicted for the $t(^{30}\text{Mg}, p)^{32}\text{Mg}$ reaction, which were rather close to the observed ones.

Assuming a beam intensity on target of $10^5/\text{s}$ for ^{44}Ar and using the cross-section estimate from our DWBA calculations (using spectroscopic amplitudes of 1) together with the known efficiencies of our detection system we arrive at the rate estimates tabulated in Table 1. In addition, we can measure the (t, d) reaction products at the same time and get additional information on the intermediate nucleus ^{45}Ar . The cross sections for this reaction are about 20-70 mb. So about 70 - 260 deuterons/h can be expected from the $t(^{44}\text{Ar}, d)^{45}\text{Ar}$ reaction. This will allow to gate on γ rays detected by the MINIBALL detector and further reduce the background. Due to the negative Q-value the deuterons will only be observed in forward direction in the laboratory frame and thus do not disturb our proton identification in backward direction.

We simulated the angular distributions for the (t, p) reaction with the statistics to be expected and compared them to the ideal theoretical angular distributions. Fig. 6 shows the efficiency and solid angle corrected angular distribution as a function of laboratory angle for the $t(^{44}\text{Ar}, p)^{46}\text{Ar}$ reaction corresponding to 10 days of beam time. For the analysis of the simulation shown in Fig. 5 the same method as for the $t(^{30}\text{Mg}, p)^{32}\text{Mg}$

Reaction	E_{state} [keV]	J^π	σ [mb]	counts/h
$t(^{44}\text{Ar}, p)^{46}\text{Ar}$	0	0^+	0.6	2.2
	1570	2^+	1.0	3.6
	2710	0^+	1.1	4.0
	3892	4^+	2.3	8.3
	total		5	18
$t(^{44}\text{Ar}, d)^{45}\text{Ar}$	0	$(7/2^-)$	72	260
	550	$(3/2^-)$	30	108
	1420	$(3/2^-)$	21	75
	total		123	443

Table 1: Expected count rates for the $t(^{44}\text{Ar}, p)^{46}\text{Ar}$ and $t(^{44}\text{Ar}, d)^{45}\text{Ar}$ reactions.

reaction has been applied. It can be seen that the different angular momentum transfer ΔL can be clearly identified by their shape.

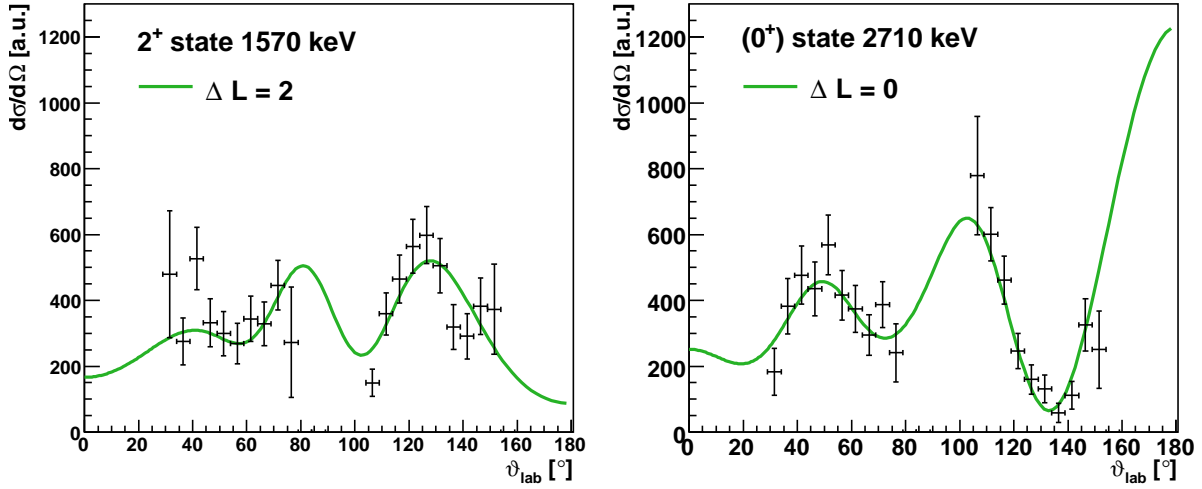


Figure 6: Efficiency and solid angle corrected angular distribution for the simulation shown in Fig. 5. The same analysis as for the $t(^{30}\text{Mg}, p)^{32}\text{Mg}$ reaction shown in Fig. 1 has been performed.

We request in total 30 shifts (10 days) of beam time with ^{44}Ar . Additionally, we ask for 3 shifts to prepare the beam.

References

- [1] O. Sorlin, M.G. Porquet, Prog. Part. Nucl. Phys. 61, 602 (2008).
- [2] S. Grévy, et al., Eur. Phys. J. A 25, s01, 111 (2005).
- [3] L. Gaudefroy, et al., Phys. Rev. C 78, 034307 (2008).

- [4] H. Scheit et al., Phys. Rev. Lett. 77, 3967 (1996).
- [5] Zs. Dombrádi et al., Nucl. Phys. A 727, 195 (2003).
- [6] L. A. Riley, Phys. Rev. C 72, 024311 (2005).
- [7] S. Bhattacharyya, et al. Phys. Rev. Lett. 101, 032501 (2008).
- [8] D. Mengoni et al., Acta. Phys. Pol. B40, 485 (2009).
- [9] M. Zielińska et al., Phys. Rev. C 80, 014317 (2009).
- [10] V. Bildstein et al., Prog. Nucl. Part. Phys. 59, 386 (2007).
- [11] I. J. Thompson, Comput. Phys. Rep. 7, 167 (1988).
- [12] H. Feshbach, “Theoretical Nuclear Physics: Nuclear Reactions” (Wiley, 1992).
- [13] M. Mahgoub, PhD Thesis, TU München, 2008.
- [14] E. R. Flynn et al., Nucl. Phys. A 246 (1975) 117.
- [15] L. Penescu et al., International Conference on Ion Sources, Gatlinburg, Tennessee (2009) and T. Story, private communication.
- [16] Th. Otto (CERN, SC-RP), Official Memorandum to ISOLDE Physics Coordinator (2007).
- [17] C. M. Perey and F. G. Perey, Atom. Data and Nucl. Data. Tables 17, 1 (1976).
- [18] G. Audi, A. H. Wapstra and C. Thibault, Nucl. Phys. A 729, 337 (2003).
- [19] <http://geant4.web.cern.ch/geant4/>